

Design and Optimization of Tubular Permanent Magnet Linear Motor for Electric Power Steering System

Hamidreza Akhondi¹ and Jafar Milimonfared²

¹ Department of Electrical Engineering, Amirkabir University of Technology, Iran, akhondi@aut.ac.ir

² Department of Electrical Engineering, Amirkabir University of Technology, Iran, monfared@aut.ac.ir

Abstract

Recent advances in Electric Power Steering technology have promised significant improvements in vehicle handling performance and safety. Electric power steering is a new kind of power steering which is developing rapidly these years due to their superior energy efficiency and energy conservation. This paper presents a possible design solution of an electric power steering actuator for hybrid electric vehicles. The design criteria of a tubular linear motor with interior permanent magnet are described and a tubular interior permanent magnet linear motor is designed and optimized with respect to weight and force ripple for Electric Power Steering application. Such an application requires low motor vibration and low force fluctuations which are considered in design process. A finite element analysis is used to validate the results obtained from the analytical model, comparing the magnetic field quantities as well as the mechanical force.

Keywords

electric power steering, finite element analysis, optimization, simulated annealing method, tubular permanent magnet linear motor

1. INTRODUCTION

The electric power steering system (EPS) is a significant contribution to the steering system since the introduction of hydraulic power steering. The advantages provided by EPS, compared to hydraulic power steering, include: ability to tune steering feel, modularity and easy assembly, compact size, engine independence and fuel economy and environmental friendliness [Badawy et al., 2000].

The basic design of automotive steering systems has changed little since the invention of the steering wheel: the driver's steering input is transmitted by a shaft through some type of gear reduction mechanism (most commonly rack and pinion or recirculating ball bearings) to generate steering motion at the front wheels. One of the more prominent developments in the history of the automobile occurred in the 1950s when hydraulic power steering assist was first introduced. Since then, power assist has become a standard component in modern automotive steering systems. Using hydraulic pressure supplied by an engine-driven pump, power steering amplifies and supplements the driver-applied torque at the steering wheel so that steering effort is reduced. In addition to improved comfort, reducing steering effort has important safety implications as well, such as allowing a driver to more easily swerve to avoid an accident. The recent

introduction of electric power steering in production vehicles eliminates the need for the hydraulic pump. Electric power steering is more efficient than conventional power steering, since the electric power steering motor only needs to provide assist when the steering wheel is turned, whereas the hydraulic pump must run constantly. The assist level is also easily tuneable to the vehicle type, road speed, and even driver preference [McCann, 2000]. An added benefit is the elimination of environmental hazard posed by leakage and disposal of hydraulic power steering fluid. The range of vehicles in which EPS is used is also expanding to include those with larger engines, and so the power required for EPS motors is increasing. Nowadays EPS applies in all of electric and hybrid electric vehicles. This paper deals with the design and optimization of an interior permanent magnet (IPM) linear motor [Sebastian et al., 2004] for EPS system. A tubular type of linear motor is considered. Since the electric motor is mechanically linked to the steering rack, it should exhibit the following characteristics:

- fault-tolerant capability, especially when a steer-by-wire system is considered;
- production of smooth torque with minimum ripple, for an accurate steering control;
- high efficiency, since the electrical energy is directly provided inside the vehicle;
- Easy manufacture, because of the large number of vehicles produced every year; minimum package size and weight are further important aspects so that a linear motor with is often preferred to a direct drive system.

All these aspects have to be considered in the design and optimization of the electric motor. The IPM linear motor presents many advantages over the other motors. Among them, it exhibits high specific force, maximum acceleration, yielding a minimum size and weight, and a high efficiency, even under reduced loads. In addition, its manufacture is easy, because the PMs are simply introduced in suitable holes in the moving part. Also an IPM motor is capable to operate in flux weakening region.

2. REQUIREMENTS FOR ELECTRIC POWER STEERING

The steering rack is based on a main shaft interfacing with the tie rods and the linear electric motors. The steering rack shaft length is about 875 mm. The EPS including the motor should have an external diameter lower than 130 mm (with the case) and a total length lower than 350 mm. It is required that the steering rack has an operational range of ± 75 mm, with an operational maximum speed of 250 mm/s (for load up to 3000 N). The maximum steering-rack acceleration is 8 m/s².

A static peak force (in stall condition) of 10 kN is required during parking maneuvers. Such a force is required for at least 5 s over 1 min. The steering rack is required to sustain a continuous force of 7500 N (at a speed of 40 mm/s) for at least 180 s over 15 min. Then, a maximum dynamic force of 3000 N is required (at a speed of 200 mm/s) for at least 60 s over 4 min. It is worth noticing that high forces are required at low rack speed, whereas low forces are needed when the rack speed is high. Figure 1 reports the required peak forces at the corresponding speed of the rack by dots. Since the various forces are required at a given duty cycle, the corresponding root-mean-square (rms) forces are also shown by triangles in Figure 1.

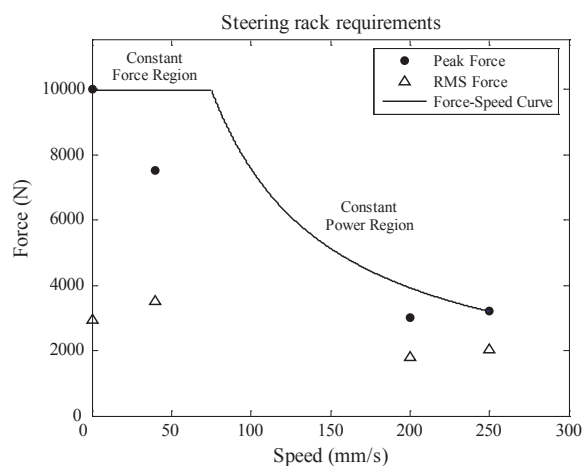


Fig. 1 Steering-rack requirement and the force versus speed curve

The electrical motor has to be designed on the basis of these rms forces. The ratio between the peak and the rms forces is almost equal to 3 for each value.

Figure 1 also shows the force versus speed curve satisfying the requirements, with a constant force region up to the speed of 75 mm/s and a constant power region up to 250 mm/s, i.e., with a speed ratio equal to 3.5. The choice of limiting the constant power region to 750 W has an immediate benefit in terms of reduced volt-ampere rating of the inverter. Since, the electrical motor has to exhibit a flux-weakening capability up to a speed ratio 3.5.

3. TUBULAR PERMANENT MAGNET LINEAR MOTOR

In recent years, linear motors have been more and more used in applications for industrial robots, machine tools, and packaging equipment, showing a significant advantage in terms of efficiency, thrust control, position accuracy, and reliability. In addition, rare-earth magnets, such as SmCo or NdFeB magnets, improve the performance of the permanent-magnet (PM) linear motor drives, making slotless motors interesting solutions. There is an increasing demand for linear servo-controlled high-speed actuation, with high precision and a high bandwidth capability [Badawy et al., 2000]. Linear electromagnetic machines, which provide thrust force directly to a payload, offer numerous advantages over their rotary to linear counterparts. Notably the absence of mechanical gears and transmission systems results in a higher dynamic performance and improved reliability. Different topologies for linear motor exist: Stator can be slotted or slot less, PMs can be surface mounted or interior and the shape of motor can be tubular or flat. Of the various linear machine topologies, tubular machines with interior permanent magnet excitation are particularly attractive since they have a high force density, capability of operation in flux weakening region and excellent servo characteristics, while having no end-windings [Chédot and Friedrich, 2003].

This paper focuses on the tubular slotted linear PM motor, including interior PM motor (TL-IPM) for electric power steering application. The linear motor should be attached to steering rack, so tubular type seems to be appropriate because of its symmetry and shape. When the stator is slotted, force density increased and EPS requirements can be obtained. As it mentioned previous IPM motors have a high force density and capability of operation in flux weakening region. However, PM motors exhibit some drawbacks: cogging forces and edge forces compromise the positional accuracy and cause oscillations and instabilities [Masada, 1995], and eccentricity increases the friction

in linear bearings, causing losses and reducing the effective force. In any case, some remedial strategies can be adopted to decrease these detent forces, for instance, by skewing or stepping the magnets, optimizing the PM widths and the axial lengths.

So a tubular slotted linear IPM motor is appropriate for electric power steering application. In the next section design and optimization of this type of linear motors for EPS application is done. EPS requirements are considered as constraints for optimization process and force to volume and force ripple are considered as objective functions. Using an idealized model of the machine, some preliminary analytical considerations are given, obtaining simple equations to have clear design indications. Then, using a more accurate model, the motor performance is investigated, as well as the dependence on the motor parameters.

4. DESIGN AND OPTIMIZATION

In this section, basic equations for TL-IPM motor are mentioned [Bianchi et al., 2003]. Using these equations we can design and optimize a TL-IPM motor for EPS application. First a simple model based on an idealized motor, which is suitable for preliminary considerations, is used. The advantages of this approach are twofold. This motor allows useful simplifications in the equations, showing the dependence of the motor performance on the main geometrical parameters. In addition, the performance of the idealized motor can be considered as references. Thus, comparing them with the performance of an actual motor, it is possible to have an idea of the quality of the latter.

With reference to Figure 2, the idealized motor is characterized by the following assumptions:

- Infinite iron permeability, so that the magnetic drop in the iron is considered null and iron losses are neglected;
- No leakage flux in the shaft diameter;
- Maximum current constrained by thermal limit, that results more restrictive than the magnetic limit (irreversible demagnetization of the magnets); this hypothesis is generally verified, since

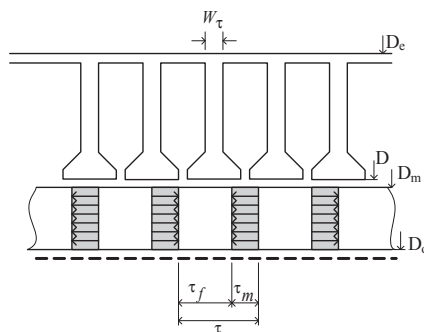


Fig. 2 Sketch of tubular linear IPM motor

the modern rare earth magnets are characterized by high coercive field even at high temperature

- A sinusoidal distribution of the electrical loading, neglecting slot and belt harmonics;
- Flux-density reaction produced by the current is neglected with respect to the PM flux density.

From the magnetic analysis of the geometry of Figure 2 [Bianchi et al., 2003], the flux-density distribution at the air gap is assumed to be a quasi-square waveform, with value expressed by following equation:

$$B_g = \frac{B_r}{2} \frac{\frac{\tau_m}{\mu_r} \left[1 - \left(\frac{D_o}{D} \right)^2 \right]}{g_{act} \left[1 - \left(\frac{D_o}{D} \right)^2 \right] + \frac{\tau_m}{\mu_r} \frac{\tau - \tau_m}{D}} \quad (1)$$

Where $g_{act} = (D - D_m)/2$ is the actual air gap, and B_r and μ_r are the PM residual flux density and differential relative permeability, respectively. Equation (1) has been computed equating D_m to D , that is, neglecting g_{act} with respect to D . In addition, the leakage fluxes in the inner part (at diameters lower than D_o) have been omitted, as by previous hypothesis. Figure 3 shows the behaviour of B_g/B_r versus τ_m/τ . Neglecting the iron

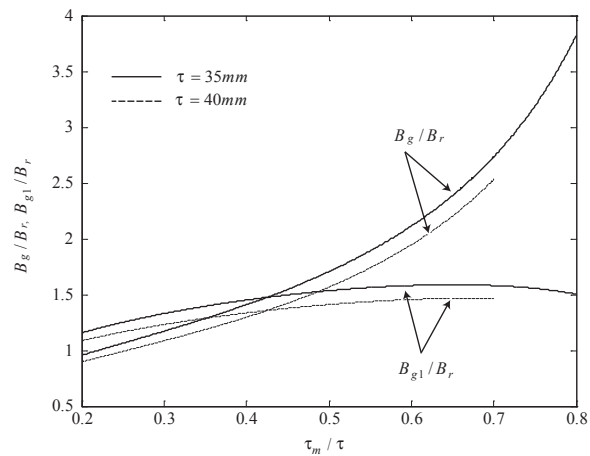


Fig. 3 Air-gap flux density in a typical tubular linear IPM motor

saturation, B_g/B_r always increases with τ_m/τ . The fundamental component of the Fourier series expansion of the air-gap flux density is an important parameter, since it is proportional to the flux linkage, and to the electromechanical force for given current; it is given by:

$$B_{g1} = \frac{4}{\pi} B_g \sin \left(\frac{\pi \tau_f}{2 \tau} \right) \quad (2)$$

Where $\tau_f = \tau - \tau_m$ has been posed. Although the flux

density B_g increases with τ_m/τ monotonically, has a maximum with respect to τ_m/τ . By putting to zero the derivative of (2) with respect to τ_m , it results in:

$$\tan\left(\frac{\pi \tau - \tau_m}{2 \tau}\right) = \frac{\pi \tau_m}{2 \tau} \frac{g_{act} + \frac{\tau_m \tau - \tau_m}{\mu_r D}}{g_{act} + \frac{\tau_m \tau_m}{\mu_r D}} \quad (3)$$

The tangent can be approximated by its argument, if the latter is small. Although the term within the parentheses is not small, adopting this approximation, the maximum of B_{g1} occurs when τ_m equals half a pole pitch. The obtained result could be a good starting point from the design point of view. The behaviour of B_{g1}/B_r versus τ_m/τ is shown in Figure 3; even if the behaviour is quite flat, its maximum point occurs at higher than 0.5.

The electrical loading is supposed sinusoidally distributed on the surface of the external part of the motor. Its value is computed from the thermal analysis, imposing the maximum temperature rise in the winding: the locked operation is taken into account, considering the Joule losses only. These are given by

$$P_{Cu} = \rho_{Cu} \pi p \tau \frac{1}{\left(1 - \frac{B_g}{B_t}\right)} \frac{D_e + D}{D_e - D} \frac{K_{sp}^2}{k_{fill}} \quad (4)$$

Where ρ_{Cu} is the copper resistivity, p is the number of pole pairs, K_{sp} is the peak value of the linear current density distribution, k_{fill} is the filling factor, and B_t is the fixed value of flux density in the tooth. The term within the parentheses corresponds to the reduction of space for the winding arrangement, due to the presence of the teeth, whose width ω , is designed on the basis of the values of the air gap and tooth flux density B_g and B_t .

The heat is transferred to the environment through the external surface ($\pi D_e 2p\tau$). The winding temperature rise ϑ_ω is related to P_{Cu} by means of the overall heat transfer coefficient, that is,

$$P_{Cu} = h \vartheta_\omega \pi D_e 2p\tau \quad (5)$$

The rated electrical loading is computed from (4) and (5), resulting in

$$K_{sp} = \sqrt{\frac{h \vartheta_\omega}{\rho_{Cu}} k_{fill} \left(1 - \frac{B_g}{B_t}\right) 2D_e \frac{D_e - D}{D_e + D}} \quad (6)$$

From (6), one can note that K_{sp} is a monotonic function of both the variable B_g and D .

The average motor force is given by:

$$F = 4pD\tau K_{sp} B_g \sin\left(\frac{\pi \tau_f}{2 \tau}\right) \quad (7)$$

The ratio between the inner and the outer diameter, D/D_e , can be optimized in order to obtain the maximum force. Figure 4 shows the force density of the tubular linear IPM motors, respectively, fixing the external diameter $D_e = 100 \text{ mm}$. The volume is computed as the external volume ($2p\tau D_e^2$), since the machine tools generally require a square external dimension.

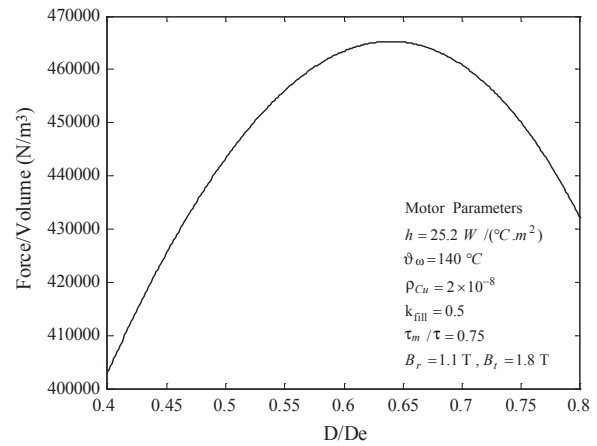


Fig. 4 Force to Volume ratio in a typical tubular linear IPM motor

The force ripple in linear motors consists of three components: (1) cogging force, interaction between the excitation flux and variable permeance of armature core due to slot openings, (2) higher harmonics of electromagnetic synchronous force and (3) higher harmonics of electromagnetic reluctance force. The controlling performance extremely drops because of the feedback of the oscillation of acceleration, velocity, and position by the ripple of driving force. Therefore, the design of lower ripple linear motor is needed for the practical utilization of EPS system.

In this paper, in order to reduce the ripple of the driving force, the optimal topology of magnet region is obtained by optimization of following objective function. The FEM calculation is performed at every 10mm displacement of magnet region in two-dimensional magneto static field. The design goal in this problem is to reduce the ripple of driving force generated on the coil region. The objective function is set as follows:

$$W = \sum_{i=1}^N \left(\frac{F_{xi} - F_T}{F_T} \right)^2 \quad (8)$$

Where N is the number of magnet positions, F_{xi} is the x -component of the electromagnetic force generated

on the coil at the magnet position i , and F_T is the target value of force.

Linear electromagnetic machines, which provide force directly to the load, offer numerous advantages over their rotary to linear counterparts. The absence of mechanical gears and transmission systems results in a higher dynamic performance and improved reliability. So for the tubular linear IPMSM, the magnetic circuit has been fully designed using the optimization from analytic and finite-element based software.

In this design, the objectives to be reached are the reduction of the volume as well as the reduction of the size of the magnets to decrease the cost [Eastham et al., 1990]. Also the force ripple is considered to be reduced by choosing the optimal dimensions for magnet shapes. An easiness of the manufacturing process must be kept in mind for a future industrial application [Zhu et al., 1997].

Taking into account the important number of design variables, an optimization under constraints is chosen. Variables are classified into discrete and continuous one. If discrete variables are fixed (for example number of stator slots) a non-linear mathematic algorithm can be used to optimize the machine structure with geometrical constraints. A number of optimization variables noted U are selected in order to find optimal values noted U^* as shown below.

U^* optimizes an objective function F and verifies the feasibility domain under constraints:

Optimize $F(U)$

$$U^* \in U$$

Subject to

$$H_i(U^*) = 0$$

$$G_i(U^*) \geq 0$$

$$U_{li} \leq U_i \leq U_{ui}$$

U^* must permit to reach the desired goal with the optimization criterion. It must also verify the equality and inequality constraints while keeping in the range of allowed values. For example, if the force to volume ratio has to be optimized, it is necessary to choose:

$U \rightarrow$ motor parameter (magnet flux linkage & dimensions)

$F(U) \rightarrow$ force to volume ratio

$G_1(U) \rightarrow$ external diameter $\leq D_{max}$ or
motor length $\leq L_{max}$

...

$G_i(U) \rightarrow$ motor force $\geq F_{min}$

In this paper, multi-objective optimization procedure is considered. The objective function is defined as following equation:

$$F(U) = \frac{F_m^a(U)}{V_{PM}^b \cdot W^c(U)} \quad (9)$$

Where F_m is motor force to volume, V_{PM} is magnet volume and W is motor force ripple function and obtain from equation (8). The relative importance of an increase in motor force density, F_m , a decrease in permanent magnet volume, V_{PM} , and a decrease in motor force ripple, W , in the design is decided by desired values of a , b and c respectively. Here, the value of $a = 1$ is chosen to simplify the design.

The method is based on an analysis and optimization parts. The analysis part uses the parametric model with the variables U to calculate the energetic values of the machine according to design specifications. The analysis part treats three domains (Figure 5). The magnetic domain is the first and the central one because it is coupled with the two others. It allows the evaluation of inductance and back-emf. This brings to electromechanical performances. The thermal domain gives temperature of magnets and copper to estimate flux density and resistances. The electrical domain gives the relationship between the current reference and the real current according to the voltage limit.

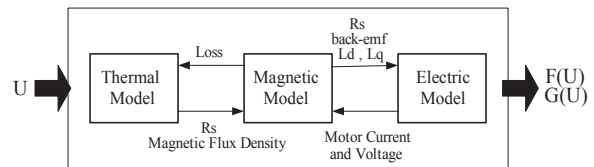


Fig. 5 Analysis module in optimization process

The optimization part manages the variables U on the basis of $F(U)$ and $G(U)$ information given by the analysis part. So a tubular interior permanent magnet linear motor is designed and optimized with respect to weight and force ripple for Electric Power Steering application. This application requires low force fluctuations and compact size which are considered in design process. A finite element analysis is used to validate the results obtained from analytical model, comparing the magnetic field quantities as well as the mechanical force. In this paper the Simulated Annealing Method (SA) is used in optimization part.

The SA algorithm mainly consists of repeating a sequence of iterations. Given an optimization problem, at a selected initial temperature, the SA starts off with the initial solutions: current and trial, randomly selected from two points within the search space. Two energy level sets of current solution and trial solution, E_i and E_j respectively, are obtained. The Metropolis algorithm, generation and acceptance is then applied. If $E_j - E_i < 0$, then the trial solution is accepted and replaces the current solution. Otherwise, the acceptance or rejection is based on Boltzmann's probability acceptance, which is $PA = \exp\left(-\frac{E_i - E_j}{KT}\right)$ where T

denotes the temperature, k is Boltzmann's constant. If PA is higher than R , where R is a random value (0-1), the trial solution is accepted and replaces the current solution. If PA is less than R then the current solution remains and a new trial solution is generated. The generation mechanism and acceptance criterion are then repeated. After a certain amount of iterations, the temperature is reduced by multiplying its value by a factor slightly below one. With reduced temperature, these two processes are repeated again until the criterion of execution is achieved [Ingber, 1993]. The final machine dimensions after optimization with this method is given in Table 1.

Table 1 Motor dimensions obtained from optimization

Motor Dimensions (Figure 2)	Value
D (mm)	65.39
D_o (mm)	8.26
D_m (mm)	66.31
D_e (mm)	102.21
τ_m (mm)	10.92
τ (mm)	18.52

Other motor parameters that have been supposed to be constant during optimization process and are chosen by considering EPS requirements are given in Table 2.

Table 2 Motor parameters

Motor Parameter	Description	Value
B_r (T)	PM residual flux density	1.23
B_t (T)	fixed value of flux density in the tooth	1.8
h (W/(°C·m ²))	overall heat transfer coefficient	24.3
ϑ_{ω} (°C)	winding temperature rise	140
ρ_{cu} (Ωm)	copper resistivity	2e-8
k_{fill}	filling factor	0.45

Table 3 compares the motor parameters such as d and q inductances, motor force, PM volume and ripple factor of initial design and optimal design. The ripple factor, R_H , of driving force is given by
$$R_H = \frac{F_{\max} - F_{\min}}{F_{\text{average}}} \times 100$$
 where F_{\max} is the maximum force, F_{\min} the minimum force, and F_{average} the average value of motor force.

It can be seen that the optimization reduces the PM volume by 21.27 %, reduces ripple factor by 62.03 % and increases the force by 16.5 %. This provides major advantages for the optimized motor over the typi-

Table 3 Motor specification comparison

	L_q/L_d	F (N)	$l_m w_m$ (mm ²)	R_H (%)
Initial design	1.86	5423.3	805.24	12.3
Optimal design	1.75	6320.3	633.90	4.67

cal motor in terms of design cost and performance.

5. FINITE ELEMENT SIMULATIONS

Finite-element (FE) optimizations of the motor design are shown in [Bianchi et al, 2001], where promising performance is emphasized.

The results obtained by this model may be compared with those of the FEM model, showing an appreciable agreement. As an example, Figure 6 shows the no-load flux plots for the slotted a tubular linear IPM motor. Figure 7 shows the Force-Velocity characteristic for designed and optimized linear motor which its parameters listed in Table 1, 2. It is obvious that this motor can satisfy the EPS requirement such as Force-Velocity characteristic (Figure 1) and EPS constraints such as motor dimensions. These items are considered as equality or inequality constraints in optimization process.

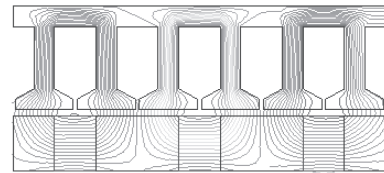


Fig. 6 No-load flux plots

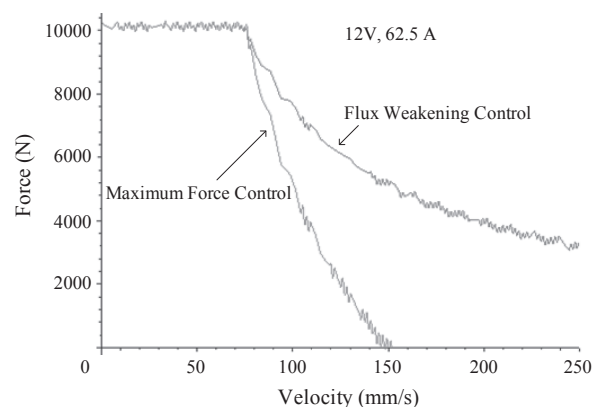


Fig. 7 Force-Velocity characteristic obtained from FEM analysis

6. CONCLUSION

In this paper, design and optimization of tubular linear interior permanent magnet motor for electric power steering application is studied. Tubular linear IPM

motors advantages in automotive systems are discussed. At first, using a simplified analytical model of the machine, some general design criteria has been found. Among them, the optimum diameter ratio and the higher force density computed for tubular linear IPM topologies. Optimization is done with different objective function such as force to volume, magnet volume and force ripple. After obtaining the motor parameters, we evaluate the performance of electric motor by finite element analysis. EPS performance can improved using a tubular linear IPM motor and drive because of its high torque density and capability of flux weakening operation.

1997.

(Received November 23, 2008; accepted August 10, 2009)

References

- Badawy, A., J. Zuraski, J. Bolourchi, and A. Chandy, Modelling and analysis of an electric power steering system, *SAE Technical Paper Series*, 1999-01-0399, 1999.
- Bianchi, N., A. Canova, G. Gruosso, M. Repetto, and F. Tonel, Analytical and finite element design optimization of a tubular linear IPM motor, *COMPEL, International Journal for Computation and Mathematics in Electrical and Electronics Engineering*, Vol. 20, No. 3, 777-795, 2001.
- Bianchi, N., S. Bolognani, D. D. Corte, and F. Tonel, Tubular linear permanent motors: an overall comparison, *IEEE Transactions on Industry Applications*, Vol. 39, No. 2, 466-475, 2003.
- Chédot, L., and G. Friedrich, Optimal control of interior permanent magnet synchronous integrated starter-generator, *Proceeding of European Power Electronics and Drive Conference*, CD-Rom, 2003.
- Eastham, J. F., R. Akmese, and H. C. Lai, Optimum design of brushless tubular linear machines, *IEEE Transaction on Magnetics*, Vol. 26, 2547-2549, 1990.
- Ingber, L., Simulated annealing: Practice versus theory, *Mathematical and Computer Modeling*, Vol. 18, 29-57, 1993.
- McCann, R., Variable effort steering for vehicle stability enhancement using an electric power steering system, *SAE Technical Paper Series*, 2000-01-0817, 2000.
- Masada, E., Linear drives for industrial applications in Japan history, existing state and future prospect, *Proceedings of LDIA95*, 9-12, 1995.
- Sebastian, T., S. Mir, and M. Islam, Electric motors for automotive applications, *EPE Journal*, Vol. 14, No. 1, 2004.
- Zhu, Z. Q., Z. P. Xia, D. Howe, and P. H. Mellor, Reduction of cogging force in slot less linear permanent magnet motors, *Proceedings of IEEE Power Electronics Application*, Vol. 144, No. 4, 277-282,